Physics Letters A 382 (2018) 1335–1340

Contents lists available at ScienceDirect

Physics Letters A

www.elsevier.com/locate/pla

Quantum-state transfer through long-range correlated disordered channels

Guilherme M.A. Almeida *, Francisco A.B.F. de Moura, Marcelo L. Lyra

Instituto de Física, Universidade Federal de Alagoas, 57072-970, Maceió, AL, Brazil

ARTICLE INFO

Article history:
Received 15 September 2017
Received in revised form 16 March 2018
Accepted 17 March 2018
Available online 21 March 2018
Communicated by A. Eisfeld

Keywords:
Quantum-state transfer
Spin chains
Correlated disorder

ABSTRACT

We study quantum-state transfer in XX spin-1/2 chains where both communicating spins are weakly coupled to a channel featuring disordered on-site magnetic fields. Fluctuations are modeled by long-range correlated sequences with self-similar profile obeying a power-law spectrum. We show that the channel is able to perform almost perfect quantum-state transmissions even in the presence of significant amounts of disorder provided the degree of those correlations is strong enough, with the cost of having long transfer times and unavoidable timing errors. Still, we show that the lack of mirror symmetry in the channel does not affect much the likelihood of having high-quality outcomes. Our results suggest that coexistence between localized and delocalized states can diminish effects of static perturbations in solid-state devices for quantum communication.

1. Introduction

Spin chains have been widely addressed as quantum channels for (especially short-distance) communication protocols since proposed in Ref. [1] that spin chains can be used for carrying out transfer of quantum information with minimal control, i.e., with no manipulation being required during the transmission process. Basically, Alice prepares and sends out an arbitrary qubit state through the channel and Bob only needs to make a measurement at some prescribed time. The evolution itself is given by the natural dynamics of the system.

Since then, several schemes for high-fidelity quantum-state transfer (QST) [1–19] and entanglement creation and distribution [20–33] in spin chains have been put forward (for reviews on the subject, see Refs. [34–36]). Perfect QST can be attained in *fully* modulated networks [2–4,37] (cf. [38,39] for proof-of-concept realizations). Other less-demanding (on the engineering side) approaches rely on optimization of the outer couplings of the chain [13] or setting *very weak* couplings between the communicating parties and the bulk of the chain [6–9,11,19,27–29] Similarly, one can also strategically apply local strong magnetic fields in order to establish resonances between the sender and receiver [16,17,23].

One factor that should be taken into account when dealing with the above protocols is disorder arising from, e.g. manufacturing errors, that could potentially damage the planned output [29,40–50]. It is known that the slightest amount of disorder is already capable of promoting Anderson localization effects [51] in 1D systems. That is not necessarily true, however, in the case of *correlated* disorder. The breakdown of Anderson localization has been reported when short- [52,53] or long-range correlations [33,54–60] are present in disordered 1D models. In particular, the latter case finds a set of extended states in the middle of the band with well detached mobility edges thereby signalling an Anderson-type metal-insulator transition [54,55]. This is also manifested in low-dimensional spin chains [33,57]. Long-range correlations with power-law spectrum can actually be found in various physical systems such as in, to name a few, DNA molecules [61], plasma fluctuations [62], patterns in surface growth [63], and graphene nanoribbons [64]. Other kinds of correlated defects have been considered in [40,42] in the context of QST.

Here, we consider a one-dimensional XX spin chain in which the local magnetic fields (on-site potentials) of the channel follow a long-range correlated disordered distribution with power-law spectrum $S(k) \propto 1/k^{\alpha}$, with k being the corresponding wave number and α being a characteristic exponent governing the degree of such correlations. We show that when perturbatively attaching two communicating (end) spins to the channel and setting their frequency to lie in the middle of the band, we are still able to perform nearly perfect QST rounds in the presence of correlated disorder, the major drawback being the requirement of long transfer times and loss of accuracy in the measurement time. Surprisingly, we find it happens even in the presence of considerable amounts of asymmetries in the channel. The reason for that is the appearance of extended states in the middle of the band which

* Corresponding author.
E-mail address: gmaalmeidaphys@gmail.com (G.M.A. Almeida).

https://doi.org/10.1016/j.physleta.2018.03.028
0375-9601/

offers the necessary end-to-end *effective* symmetry thereby supporting the occurrence of Rabi-like oscillations between the sender and receiver spins. We further show that perfect mirror symmetry is not a crucial factor as long as there exists a proper set of delocalized eigenstates in the channel.

In the following, Sec. 2, we introduce the XX spin Hamiltonian with on-site long-range correlated disorder. In Sec. 3 we derive an effective two-site Hamiltonian that accounts for the way both communicating parties are coupled to the channel. In Sec. 4 we display the results for the QST fidelity and timing errors. Our final remarks are addressed in Sec. 5.

2. Spin-chain Hamiltonian

We consider a pair of spins (communicating parties) coupled to a one-dimensional quantum channel consisting altogether of spin-1/2 chain with open boundaries featuring XX-type exchange interactions described by Hamiltonian $\hat{H} = \hat{H}_{\rm ch} + \hat{H}_{\rm int}$ with ($\hbar = 1$)

$$\hat{H}_{\rm ch} = \sum_{i=1}^{N} \frac{\omega_i}{2}(\hat{1} - \hat{\sigma}_i^z) - \sum_{\langle i,j\rangle} \frac{J_{i,j}}{2}(\hat{\sigma}_i^x\hat{\sigma}_j^x + \hat{\sigma}_i^y\hat{\sigma}_j^y), \tag{1}$$

where $\hat{\sigma}_i^{x,y,z}$ are the Pauli operators for the i-th spin, ω_i is the local (on-site) magnetic field, and $J_{i,j}$ is the exchange coupling strength between nearest-neighbor sites. Supposing the sender (s) and receiver (r) spins are connected to sites 1 and N from the channel at rates g_s and g_r, respectively, the interaction part reads

$$\hat{H}_{\rm int} = \frac{\omega_s}{2}(\hat{1} - \hat{\sigma}_s^z) + \frac{\omega_r}{2}(\hat{1} - \hat{\sigma}_r^z) - \frac{g_s}{2}(\hat{\sigma}_s^x\hat{\sigma}_1^x + \hat{\sigma}_s^y\hat{\sigma}_1^y) - \frac{g_r}{2}(\hat{\sigma}_r^x\hat{\sigma}_N^x + \hat{\sigma}_r^y\hat{\sigma}_N^y). \tag{2}$$

Note that since $\hat{H}$ conserves the total magnetization of the system, i.e., $\left[\hat{H}, \sum_i \hat{\sigma}_i^z\right] = 0$, the Hamiltonian can be split into independent subspaces with fixed number of excitations. Here we focus on the single-excitation Hilbert space spanned by the computational basis $|i\rangle = \hat{\sigma}_i^+|\downarrow\downarrow\ldots\downarrow\rangle$ with $i = r, s, 1, \ldots, N$, that means every spin pointing down but the one located at the i-th position. In this case, we end up with a hopping-like matrix with $N+2$ dimensions.

Let us now make a few assumptions in regard to the channel described by Hamiltonian (1). Here we consider the spin-exchange coupling strengths to be uniform $J_{i,j} \to J$ and, in order to study the robustness of the channel against disorder we introduce correlated static fluctuations on the on-site magnetic field ω_n, $n = 1, \ldots, N$. A straightforward way to generate random sequences featuring internal long-range correlations is through the trace of the fractional Brownian motion with power-law spectrum $S(k) \propto 1/k^{\alpha}$ [54,59]

$$\omega_n = J\sum_{k=1}^{N/2} k^{-\alpha/2}\cos\left(\frac{2\pi nk}{N} + \phi_k\right), \tag{3}$$

where $k = 1/\lambda$, is the inverse modulation wavelength, $\{\phi_k\}$ are random phases distributed uniformly within $[0, 2\pi]$, and α controls the degree of correlations. This parameter is related to the so-called Hurst exponent [65], $H = (\alpha - 1)/2$, which characterizes the self-similar character of a given sequence. When $\alpha = 0$, we recover the case of uncorrelated disorder (white noise) and for $\alpha > 0$ underlying long-range correlations take place. The resulting long-range correlated sequence becomes nonstationary for $\alpha > 1$. Furthermore, according to the usual terminology, when $\alpha > 2$ ($\alpha < 2$) the series increments become persistent (anti-persistent). Interestingly, this brings about serious consequences on the spectrum profile of the system. As shown in [54,59], when $\alpha > 2$ there occurs the appearance of delocalized states in the middle of the one-particle spectrum band. In the QST scenario with weakly-coupled spins r and s, i.e. $g_s, g_r \ll J$, that promotes a strong enhancement in the likelihood of disorder realizations with very-high fidelities F, most of them yielding $F \approx 1$. This will be elucidated along the paper.

Hereafter we set the sequence generated by Eq. (3) to follow a normalized distribution, that is $\omega_n \to (\omega_n - \langle\omega_n\rangle)/\sqrt{\langle\omega_n^2\rangle - \langle\omega_n\rangle^2}$. We also stress that such a disordered distribution has no typical length scale which is a property of many natural stochastic series [66].

3. Effective two-site description

We now work out a perturbative approach to write down a proper representation of an effective Hamiltonian involving only the sender and receiver spins provided they are very weakly coupled to the channel. Intuitively, we expect they span their own subspace with renormalized parameters and thus QST takes place via effective Rabi oscillations between them [7,19]. Our goal here is to investigate the influence of disorder in such subspaces and evaluate their resilience to imperfections in the channel.

Following a second-order perturbation approach (for details, see Refs. [7,8] or Supplementary Material), we can obtain an effective Hamiltonian projected onto $\{|s\rangle, |r\rangle\}$ which reads

$$\hat{H}_{sr} = \begin{pmatrix} h_s & -J' \\ -J' & h_r \end{pmatrix}, \tag{4}$$

with

$$h_\nu = \omega_\nu - \epsilon^2 g_\nu^2 \sum_k \frac{|a_{\nu k}|^2}{E_k - \omega_\nu}, \tag{5}$$

$\nu \in \{s, r\}$, and

$$J' = \frac{\epsilon^2 g_s g_r}{2}\sum_k \left(\frac{a_{sk}a_{rk}}{E_k - \omega_s} + \frac{a_{sk}a_{rk}}{E_k - \omega_r}\right), \tag{6}$$

where ϵ being the perturbation parameter, $a_{sk} \equiv \langle 1|E_k\rangle$, $a_{rk} \equiv \langle N|E_k\rangle$, and $\{|E_k\rangle\}$ are the eigenstates of the channel [Eq. (1)] with corresponding (nondegenerate) frequencies $\{E_k\}$. Note that we are assuming all parameters to be real.

Hamiltonian (4) describes a two-level system which performs Rabi-like oscillations in a time scale set by the inverse of the gap between its normal frequencies. In order to have as perfect as possible QST one should guarantee that $h_s = h_r$. This is automatically fulfilled, given $\omega_s = \omega_r$ and $g_s = g_r = g$, for mirror-symmetric chains since $|a_{sk}| = |a_{rk}|$ for every k. In that case, for a noiseless uniform channel and in the limit of very weak outer couplings, which implies in the validity of Hamiltonian (4), an initial state prepared in $|s\rangle$ will evolve in time to $|r\rangle$ with nearly unit amplitude at times $\tau = n\pi/(2J') = n\pi J/(2\epsilon^2 g^2)$, with n being an odd integer [6,7]. Note that as N increases more eigenstates get in the middle of the spectrum and thus ϵg_ν must be adjusted accordingly (we shall drop out the perturbation parameter ϵ hereafter).

4. Quantum-state transfer protocol

4.1. General scheme

In the standard QST procedure [1], Alice is able to control the spin located at position s and wants to send an arbitrary qubit $|\phi\rangle_s = \alpha|\downarrow\rangle_s + \beta|\uparrow\rangle_s$ to Bob which has access to spin r. Now let us assume that the rest of the chain is initialized in the fully polarized spin-down state so that the whole state reads

$|\Psi(0)\rangle = |\phi\rangle_s|\downarrow\rangle_1 \ldots |\downarrow\rangle_N|\downarrow\rangle_r$. She then let the system evolve following its natural dynamics, $|\psi(t)\rangle = \hat{\mathcal{U}}(t)|\psi(0)\rangle$, where $\hat{\mathcal{U}}(t) \equiv e^{-i\hat{H}t}$ is the unitary time-evolution operator. Ideally, she expects that at some prescribed time τ the evolved state takes the form $|\Psi(\tau)\rangle = |\downarrow\rangle_s|\downarrow\rangle_1 \ldots |\downarrow\rangle_N|\phi\rangle_r$. At this point, Bob receives state $\rho_r(\tau) = \mathrm{Tr}_{s,1,\ldots,N}|\Psi(\tau)\rangle\langle\Psi(\tau)|$ and thus the transfer fidelity can be evaluated by $F_\phi(\tau) = \langle\phi|\rho_r(\tau)|\phi\rangle$. Note, however, that this measures the performance of QST for a specific input. In order to properly evaluate the efficiency of the *channel*, we may average the above quantity over all input states $|\phi\rangle_s$ (that is, over the Bloch sphere) which results in [1]

$$F(t) = \frac{1}{2} + \frac{f_r(t)}{3} + \frac{f_r(t)^2}{6} \tag{7}$$

for an arbitrary time with $f_i(t) \equiv |\langle i|e^{-i\hat{H}t}|s\rangle|$. Therefore, we note that such a state-independent figure of merit of QST depends solely upon the transition amplitude between the sender and receiver spins with $F(t) = 1$ only when $f_r(t) = 1$. The problem of transmitting a qubit state from one point to another can thus be viewed as a single-particle continuous quantum walk [67] on a network and the goal is to find out ways to transfer the excitation between two distant sites with the highest possible transition amplitude.

4.2. Results

In the case of weakly-coupled spins in which an effective two-site interaction sets in [cf. Eq. (4)], the transition amplitude $f_r(t)$ will strongly depend upon $\Delta \equiv h_s - h_r$. The emergence of long-range correlations should then favor smaller values of Δ (see Supplementary Material for a discussion about this).

Now, let us see about the resulting QST performance. As a testbed, we consider a $N = 50$ channel, $g_\nu = g = 0.001J$, and $\omega_\nu = 0$. Given the size of the channel, this chosen value for g assures that the subspace created by states $|s\rangle$ and $|r\rangle$ becomes safely shielded from influence of channel normal modes lying around the band center. Even if one of them gets close by, it is very likely that the eigenstate will not be extremely asymmetric due to the presence of delocalized states for high enough α (see Supplementary Material).

In Fig. 1 we show the sample distribution of the maximum fidelity $F_{\max} = \max\{F(t)\}$ [as defined above in Eq. (7)] achieved in time interval $t \in [0, 20\tau]$, with $\tau = \pi J/(2g^2)$ being the corresponding time for which a complete transfer would occur for the noiseless case, $f_r(\tau) \approx 1$, as seen in Sec. 3. That interval is a pretty reasonable one in order to guarantee at least one full Rabi cycle in most of the samples. Recall that the effective sender-receiver hopping strength J' dictates the time scale of the dynamics and is strongly affected by disorder. Fig. 1 shows that strong long-range correlations in the disorder distribution enhances the figure of merit of QST enormously. Even more impressive is the fact that, for $\alpha = 2$ and $\alpha = 3$ [see Figs. 1(c) and 1(d), respectively], we find the number of occurrences of fidelities $F_{\max} \approx 1$ to be the highest one. We also note that the fidelities for $\alpha = 2$ case [Fig. 1(c)] are fairly well distributed across all the possible outcomes, thus indicating a transition regime.

In order to provide an explicit view on what is actually going on in the QST process, in Fig. 2(a) we show the time evolution of the occupation probabilities $f_i^2(t)$ of the sender ($i = s$), receiver ($i = r$), and channel [$f_{\mathrm{ch}}^2(t) \equiv \sum_{n=1}^{N} f_n^2(t)$] spins for one particular (ordinary) sample, out of many successful ones (meaning $F_{\max} \approx 1$) encountered for $\alpha = 3$ [see Fig. 1(d)]. There we see a genuine Rabi-like behavior yielding a very high-quality QST. We reduced the time scale to 2τ so we can have a more detailed view on a

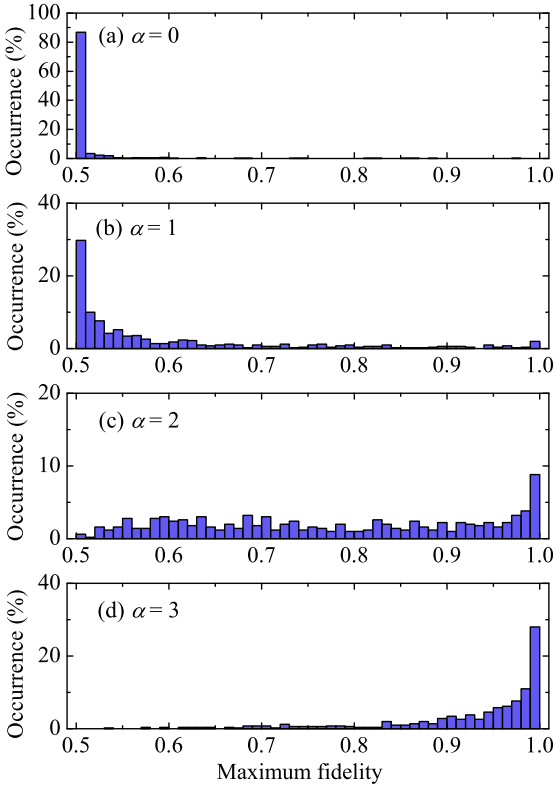

Fig. 1. (Color online.) Maximum-fidelity histogram for 500 independent realizations of disorder for $\alpha = 0, 1, 2$, and 3. Results were obtained from exact numerical diagonalization of the full Hamiltonian $\hat{H} = \hat{H}_{\mathrm{ch}} + \hat{H}_{\mathrm{int}}$ with $N = 50$, ω_n, $n = 1, \ldots, N$, given by Eq. (3), $\omega_\nu = 0$, and $g_\nu = g = 0.001J$. The maximum fidelity $F_{\max} = \max\{F(t)\}$ [see Eq. (7)] was registered during time interval $[0, 20\tau]$, with $\tau = \pi J/(2g^2)$.

complete cycle. Therefore, in this case the transfer time happens to be roughly the same as for the noiseless case. Furthermore, we note that the channel is barely populated for all practical purposes [see the inset of Fig. 2(a)], meaning that Eq. (4) is a robust approximation. Those residual beatings seen for $f_{\mathrm{ch}}^2(t)$ are due to some negligible mixing between both channel and sender/receiver subspaces. One could get rid of it by further decreasing g. Care must be taken, though, not to compromise the transfer time scale since it goes as $\sim 1/g^2$.

Fig. 2(b) shows the corresponding spatial distribution of eigenstates, $|\langle i|\psi_k\rangle|^2$, along the whole spectrum k. First, note that the outer parts of the spectrum are mostly populated by localized-like eigenstates [54]. Indeed, the eigenstates get more delocalized as we move towards the center of the band [see Supplementary Material]. We also point out the asymmetrical aspect of the eigenstate distribution. Still, it turns out to be possible to span an independent subspace involving only the sender and receiver spins [Eq. (4)] so that their corresponding eigenstates become close to $(|s\rangle \pm |r\rangle)/\sqrt{2}$. We shall also remark that although we have set the sender and receiver frequencies to the very center of the band, that is $\omega_s = \omega_r = 0$, this pair of eigenstates responsible for the Rabi-like dynamics of the system might be slightly shifted around that region due to the lack of particle-hole symmetry in the channel. That, however, does not compromise the efficiency of the transfer. By looking closely at Fig. 2(b), we spot many eigenstates showing strong asymmetries between spins 1 and N. Fortunately, since a_{sk} and a_{rk} are fairly balanced across the spectrum and due to the fact that the channel eigenstates lying around the middle of the band (less asymmetric) have great influence on Δ/J', given that the terms in the sum in Eqs. (5) and (6) go as $\sim 1/E_k$, the sender and receiver spins are able to find a way out through such asymme-

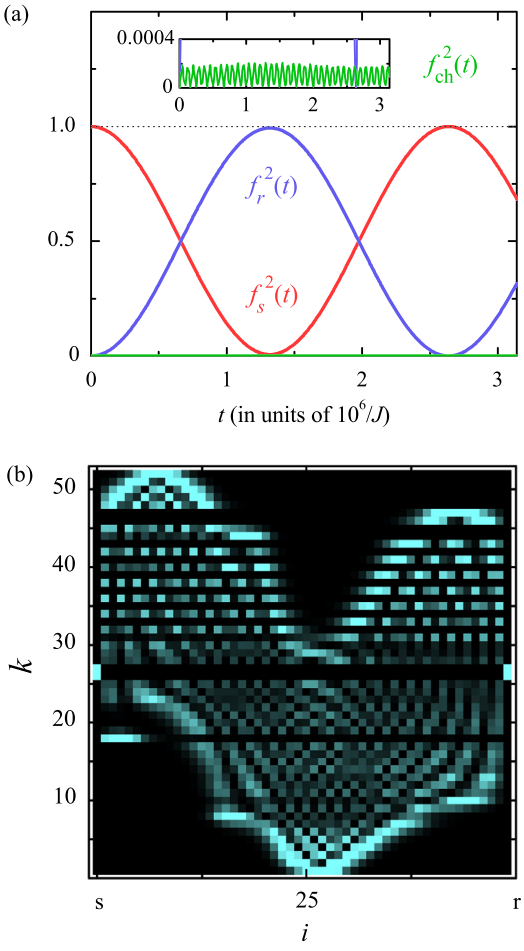

Fig. 2. (Color online.) (a) Time evolution of the occupation probability amplitudes for the sender $f_s^2(t)$, receiver $f_r^2(t)$, and channel spins, the latter being the sum of the amplitudes within the channel, namely $f_{\rm ch}^2(t) \equiv \sum_{n=1}^{N} f_n^2(t)$. For this particular realization, we simply took one of the samples which provided $F_{\rm max} \approx 1$ in Fig. 1(d) for $\alpha = 3$. Note that the time scale has been reduced to twice the transfer time for the noiseless case, that is 2τ, for a better view of a Rabi-like cycle. The inset shows the very same graph but for a much smaller scale of amplitude in order to account for the (rather negligible) behavior of $f_{\rm ch}^2(t)$. (b) Corresponding density plot of the eigenstate spatial distribution $|\langle i|\psi_k\rangle|^2$ for every k (in increasing order of energy). Darker (brighter) spots indicate lower (higher) overlaps. Note the formation of a pair of states in the middle of the band with strong overlap in $|s\rangle$ and $|r\rangle$ simultaneously. These are the source of such high-fidelity QST rounds. System's parameters: $N = 50$, $\omega_v = 0$, and $g_v = 0.001\,J$.

tries and establish an effective resonant interaction between them thus resulting in an almost perfect QST for most of the samples.

Now, in order to evaluate a representative outcome for $F_{\rm max}$ for a given α, in Fig. 3 we plot its average over all the samples for a large window of α values. This clearly illustrates the overall behavior of the occurrences of $F_{\rm max}$ as one increases the degree of long-range correlations in the disorder distribution. Note that we are also showing the curve for many values of g, only to stress the importance of setting this parameter as smaller as possible so as to avoid mixing between the channel and sender/receiver subspaces. Indeed, the performance quality of QST is affected by that. As we go towards smaller values of g, there is a saturation point indicating that Hamiltonian (4) has reached its final form. It means that if we keep on decreasing g, the QST fidelity will not get any better and the time scale of the transfer will increase substantially. Furthermore, we identify in Fig. 3 that the $F_{\rm max}$ growth profile is more pronounced between $\alpha = 1$ and $\alpha = 3$ until it saturates for higher values of α. This is associated to the fact that the long-range correlated sequence generated by Eq. (3) becomes nonstationary for

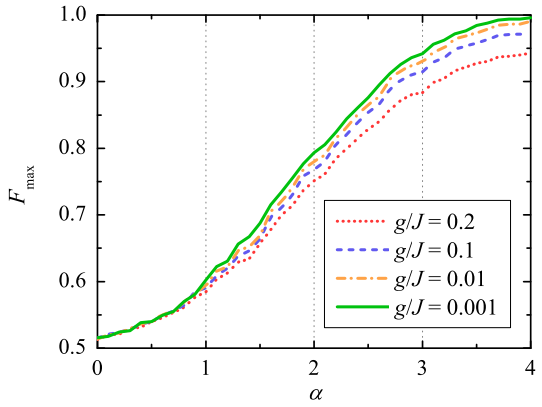

Fig. 3. (Color online.) Maximum fidelity versus α averaged over 500 independent disorder realizations. Now, we have set $g/J = 0.001$, 0.01, 0.1, and 0.2, while other system's parameters were kept as usual, namely $N = 50$ and $\omega_v = 0$. The maximum fidelity $F_{\rm max} = \max\{F(t)\}$ for each sample was again obtained during time interval $[0, 20\tau]$, with $\tau = \pi J/(2g^2)$.

$\alpha > 1$ and acquires persistent character when $\alpha > 2$, thereby triggering the appearance of delocalized states in the middle of the band [54,59].

4.3. Measurement-time issues

So far, we have been concerned with the quality of QST, that is, the channels' capability of generating an effective Rabi dynamics between the outer spins even when subjected to a certain class of on-site fluctuations. That was carried out by evaluating the fidelity statistics over a given time interval. It happens to be very relevant on its own the fact that, eventually, one should be able retrieve the state with $F \approx 1$ in an increasing number of samples when $\alpha \geq 2$ (see Fig. 1). For practical implementations, though, a rather precise measurement time is required. At this point, we must stress that disorder, in general, besides being detrimental to the QST fidelity, also makes it trickier (if not impossible) to predict the exact time (or, at least, a proper time window) at which the state is supposed to reach the desired location with highest probability. Still, in this last part of our discussion, let us address the above timing issue.

As pointed out earlier, the transfer time for a noiseless, uniform channel operating in the off-resonant regime is $\tau = \pi J/(2g^2)$ [6]. For an arbitrary channel one should have $\tau' = \pi/(2|J'|)$, with (recalling) J' being the effective coupling between spins s and r, determined by g and the sum in Eq. (6). Note that even if a given sample does yield a very small Δ/J' – which happens quite often for $\alpha \geq 3$ – thus allowing for very high fidelities, it is likely that J' itself will have been shifted due to fluctuations in the spectrum of the channel, thus altering the time scale of the dynamics. Now, given the circumstances, what we can do is to evaluate, given a *threshold* for the transfer quality, the fraction of samples assured to keep the original, prescribed measurement time τ and/or access how much it deviates from that. In Fig. 4 we show the above for $F(\tau') > 0.95$ and $F(\tau') > 0.99$ against various times τ' (in units of τ) and for $\alpha = 3$, 3.5, and 4. We note that the largest fractions of successful QST outcomes happens at times of the order of τ. This becomes even more prominent when $\alpha = 4$ for which it displays a Gaussian-like profile around $\tau'/\tau = 1$, reaching about a 45% (15%) chance of retrieving the state at the original time with fidelities above 0.95 (0.99) [compare Figs. 4(a) and 4(b)]. One should also note it shrinks upon increasing the fidelity threshold. This is a direct consequence of featuring a large number of outcomes occurring around the same time spot. In Rabi-like QST protocols, the fidelity evolves periodically following $f_r(t) \simeq \sin(J't)$ – just like in a two-level system – and so, picturing out a complete cycle in

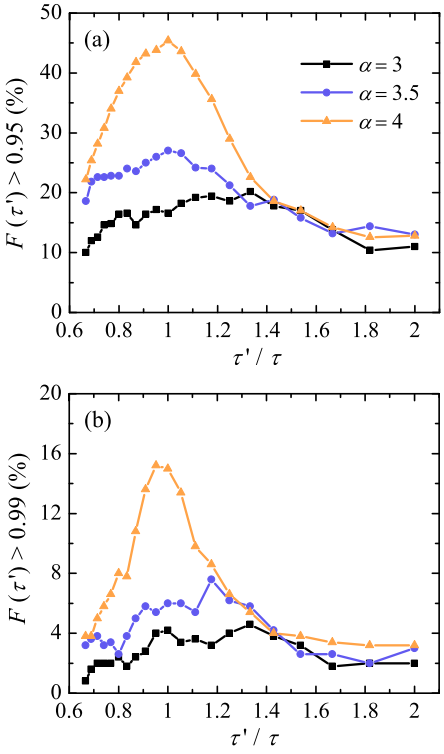

Fig. 4. Fraction (%) of samples displaying (a) $F(\tau') > 0.95$ and (b) $F(\tau') > 0.99$ versus τ'/τ, with $\tau' = \pi/(2|J'|)$ and $\tau = \pi J/(2g^2)$ being the measurement time for the noiseless case. We considered 500 independent realizations of disorder with $\alpha = 3$, 3.5, and 4 in both panels. Results were obtained from exact numerical diagonalization of the full Hamiltonian $\hat{H}$ [cf. Eqs. (1) and (2)] for $N = 50$, $g_v = 0.01J$, and $\omega_v = 0$. We show the time interval featuring the most relevant outcomes, though there is a finite (small) possibility of finding successful transfers at longer times.

time, that is what should happen as we go towards the top of the peak.

5. Concluding remarks

We studied a QST protocol through a XX spin channel with on-site long-range-correlated disorder. The protocol involved a couple of communicating spins weakly coupled to the channel not matching with any of its normal modes so that the transfer takes place through Rabi-like oscillations between the ends of the chain [6,7,19]. We focused on the reduced sender/receiver description based on Hamiltonian (4) which embodies all the relevant information regarding the way they are affected by the channel, thus allowing one to foresee the QST outcome based on the renormalized parameters contained in the two-site effective Hamiltonian.

We showed that this class of weakly-coupled models are indeed robust against external perturbations [45] as the effective interaction between sender and receiver spins do not depend upon the entire wavefunction of the spectrum but rather on the local amplitudes of the spins they are connected to. Because of that, we realize we do not necessarily need a perfect symmetric chain to achieve an almost perfect QST. When scale-free correlations with a power-law spectral density $S(k) \propto k^{-\alpha}$ set in, the disorder distribution is such that it can support delocalized eigenstates around the center of the band [54]. Those are able to provide a broader, more balanced distribution of amplitudes even in the presence of asymmetries, what makes it possible to induce effective resonant interactions between $|r\rangle$ and $|s\rangle$, provided α is high enough. We stress, however, that this class of weak-coupling models [6,7] should find practical limitations (especially for large chains) for they usually require long transfer times. Also, disorder, in general, promotes fluctuations in the measurement time, which is another source of errors.

It is worthwhile to highlight the crucial role of the intrinsic correlations in the disorder distribution in the performance of QST. As the correlation degree α increases in Eq. (3) the on-site probability distribution goes from a Gaussian to a bimodal profile. This variation on the probability distribution on its own, however, does not imply in the improvement of the QST fidelity. We verified this by generating a correlated sequence $\{\omega_n\}$ followed by a random shuffling of the site energies. This very simple procedure destroys the intrinsic correlations but maintains the very same probability distribution overall. Then, we observed that the withdrawal of correlations yielded $F(t) \approx 0.5$ for the same range of α values as in Fig. 3 thus ruling out any possibility of carrying out the quantum-state transfer protocol. Indeed, the main ingredient definitely turns out to be the intrinsic correlations within the disorder distribution.

Note that we have not considered the case of structural disorder here, that is, fluctuations on the spin couplings. However, on-site disorder actually embodies a worst-case scenario since the channel also looses its particle-hole symmetry, differently from spin-coupling disorder.

We remark that disorder, correlated or not, might arise naturally due to experimental imperfections in the manufacturing process of solid state devices for quantum information processing and thus finding out was to prevent and/or deal with that becomes of great relevance. Here we have seen that long-range correlated disorder is not so detrimental to the transfer process as the uncorrelated counterpart. This further promotes the investigation of the effects of other particular kinds of fluctuations in the transport of quantum information.

Acknowledgements

We thank T. Apollaro for valuable conversations. This work was partially supported by CNPq (Grant No. 152722/2016-5), CAPES, FINEP, and FAPEAL (Brazilian agencies).

Appendix A. Supplementary material

Supplementary material related to this article can be found online at https://doi.org/10.1016/j.physleta.2018.03.028.

References

[1] S. Bose, Phys. Rev. Lett. 91 (2003) 207901.
[2] M. Christandl, N. Datta, A. Ekert, A.J. Landahl, Phys. Rev. Lett. 92 (2004) 187902.
[3] M.B. Plenio, J. Hartley, J. Eisert, New J. Phys. 6 (2004) 36.
[4] G.M. Nikolopoulos, D. Petrosyan, P. Lambropoulos, Europhys. Lett. 65 (2004) 297.
[5] T.J. Osborne, N. Linden, Phys. Rev. A 69 (2004) 052315.
[6] A. Wójcik, T. Łuczak, P. Kurzyński, A. Grudka, T. Gdala, M. Bednarska, Phys. Rev. A 72 (2005) 034303.
[7] A. Wójcik, T. Łuczak, P. Kurzyński, A. Grudka, T. Gdala, M. Bednarska, Phys. Rev. A 75 (2007) 022330.
[8] Y. Li, T. Shi, B. Chen, Z. Song, C.-P. Sun, Phys. Rev. A 71 (2005) 022301.
[9] M.X. Huo, Y. Li, Z. Song, C.P. Sun, Europhys. Lett. 84 (2008) 30004.
[10] J. Liu, G.-F. Zhang, Z.-Y. Chen, Phys. Lett. A 372 (2008) 2830.
[11] G. Gualdi, V. Kostak, I. Marzoli, P. Tombesi, Phys. Rev. A 78 (2008) 022325.
[12] Z.-M. Wang, M. Byrd, B. Shao, J. Zou, Phys. Lett. A 373 (2009) 636.
[13] L. Banchi, T.J.G. Apollaro, A. Cuccoli, R. Vaia, P. Verrucchi, Phys. Rev. A 82 (2010) 052321.
[14] L. Banchi, T.J.G. Apollaro, A. Cuccoli, R. Vaia, P. Verrucchi, New J. Phys. 13 (2011) 123006.
[15] T.J.G. Apollaro, L. Banchi, A. Cuccoli, R. Vaia, P. Verrucchi, Phys. Rev. A 85 (2012) 052319.
[16] S. Lorenzo, T.J.G. Apollaro, A. Sindona, F. Plastina, Phys. Rev. A 87 (2013) 042313.
[17] S. Paganelli, S. Lorenzo, T.J.G. Apollaro, F. Plastina, G.L. Giorgi, Phys. Rev. A 87 (2013) 062309.
[18] S. Lorenzo, T.J.G. Apollaro, S. Paganelli, G.M. Palma, F. Plastina, Phys. Rev. A 91 (2015) 042321.

[19] G.M.A. Almeida, F. Ciccarello, T.J.G. Apollaro, A.M.C. Souza, Phys. Rev. A 93 (2016) 032310.
[20] L. Amico, A. Osterloh, F. Plastina, R. Fazio, G. Massimo Palma, Phys. Rev. A 69 (2004) 022304.
[21] M.B. Plenio, F.L. Semião, New J. Phys. 7 (2005) 73.
[22] T.J.G. Apollaro, F. Plastina, Phys. Rev. A 74 (2006) 062316.
[23] F. Plastina, T.J.G. Apollaro, Phys. Rev. Lett. 99 (2007) 177210.
[24] T.J. Apollaro, A. Cuccoli, A. Fubini, F. Plastina, P. Verrucchi, Phys. Rev. A 77 (2008) 062314.
[25] V. Subrahmanyam, A. Lakshminarayan, Phys. Lett. A 349 (2006) 164.
[26] T.S. Cubitt, J.I. Cirac, Phys. Rev. Lett. 100 (2008) 180406.
[27] L. Campos Venuti, S.M. Giampaolo, F. Illuminati, P. Zanardi, Phys. Rev. A 76 (2007) 052328.
[28] S.M. Giampaolo, F. Illuminati, Phys. Rev. A 80 (2009) 050301.
[29] S.M. Giampaolo, F. Illuminati, New J. Phys. 12 (2010) 025019.
[30] G. Gualdi, S.M. Giampaolo, F. Illuminati, Phys. Rev. Lett. 106 (2011) 050501.
[31] M.P. Estarellas, I. D'Amico, T.P. Spiller, Phys. Rev. A 95 (2017) 042335.
[32] M.P. Estarellas, I. D'Amico, T.P. Spiller, Sci. Rep. 7 (2017) 42904.
[33] G.M.A. Almeida, F.A.B.F. de Moura, T.J.G. Apollaro, M.L. Lyra, Phys. Rev. A 96 (2017) 032315.
[34] A. Kay, Int. J. Quantum Inf. 08 (2010) 641.
[35] T.J.G. Apollaro, S. Lorenzo, F. Plastina, Int. J. Mod. Phys. B 27 (2013) 1345035.
[36] G.M. Nikolopoulos, I. Jex (Eds.), Quantum State Transfer and Network Engineering, Springer-Verlag, Berlin, 2014.
[37] D.L. Feder, Phys. Rev. Lett. 97 (2006) 180502.
[38] M. Bellec, G.M. Nikolopoulos, S. Tzortzakis, Opt. Lett. 37 (2012) 4504–4506.
[39] R.J. Chapman, M. Santandrea, Z. Huang, G. Corrielli, A. Crespi, M.-H. Yung, R. Osellame, A. Peruzzo, Nat. Commun. 7 (2016) 11339.
[40] G. De Chiara, D. Rossini, S. Montangero, R. Fazio, Phys. Rev. A 72 (2005) 012323.
[41] J. Fitzsimons, J. Twamley, Phys. Rev. A 72 (2005) 050301.
[42] D. Burgarth, S. Bose, New J. Phys. 7 (2005) 135.
[43] D.I. Tsomokos, M.J. Hartmann, S.F. Huelga, M.B. Plenio, New J. Phys. 9 (2007) 79.
[44] D. Petrosyan, G.M. Nikolopoulos, P. Lambropoulos, Phys. Rev. A 81 (2010) 042307.
[45] N.Y. Yao, L. Jiang, A.V. Gorshkov, Z.-X. Gong, A. Zhai, L.-M. Duan, M.D. Lukin, Phys. Rev. Lett. 106 (2011) 040505.
[46] A. Zwick, G.A. Álvarez, J. Stolze, O. Osenda, Phys. Rev. A 84 (2011) 022311.
[47] A. Zwick, G.A. Álvarez, J. Stolze, O. Osenda, Phys. Rev. A 85 (2012) 012318.
[48] M. Bruderer, K. Franke, S. Ragg, W. Belzig, D. Obreschkow, Phys. Rev. A 85 (2012) 022312.
[49] S. Ashhab, Phys. Rev. A 92 (2015) 062305.
[50] A. Kay, Phys. Rev. A 93 (2016) 042320.
[51] P.W. Anderson, Phys. Rev. 109 (1958) 1492–1505.
[52] J.C. Flores, J. Phys. Condens. Matter 1 (1989) 8471.
[53] P. Phillips, H.-L. Wu, Science 252 (1991) 1805–1812.
[54] F.A.B.F. de Moura, M.L. Lyra, Phys. Rev. Lett. 81 (1998) 3735–3738.
[55] F.M. Izrailev, A.A. Krokhin, Phys. Rev. Lett. 82 (1999) 4062–4065.
[56] U. Kuhl, F.M. Izrailev, A.A. Krokhin, H.-J. Stöckmann, Appl. Phys. Lett. 77 (2000) 633–635.
[57] R.P.A. Lima, M.L. Lyra, E.M. Nascimento, A.D. de Jesus, Phys. Rev. B 65 (2002) 104416.
[58] F.A.B.F. de Moura, M.D. Coutinho-Filho, E.P. Raposo, M.L. Lyra, Phys. Rev. B 66 (2002) 014418.
[59] F. Domínguez-Adame, V.A. Malyshev, F.A.B.F. de Moura, M.L. Lyra, Phys. Rev. Lett. 91 (2003) 197402.
[60] I.F. Herrera-González, J.A. Méndez-Bermúdez, F.M. Izrailev, Phys. Rev. E 90 (2014) 042115.
[61] C.-K. Peng, S.V. Buldyrev, A.L. Goldberger, S. Havlin, F. Sciortino, M. Simons, H.E. Stanley, Nature 356 (1992) 168–170.
[62] B.A. Carreras, B. van Milligen, M.A. Pedrosa, R. Balbín, C. Hidalgo, D.E. Newman, E. Sánchez, M. Frances, I. García-Cortés, J. Bleuel, M. Endler, S. Davies, G.F. Matthews, Phys. Rev. Lett. 80 (1998) 4438–4441.
[63] C.-H. Lam, L.M. Sander, Phys. Rev. Lett. 69 (1992) 3338–3341.
[64] G.P. Zhang, M. Gao, Y.Y. Zhang, N. Liu, Z.J. Qin, M.H. Shangguan, J. Phys. Condens. Matter 24 (2012) 235303.
[65] J. Feder, Fractals, Plenum Press, New York, 1988.
[66] M. Paczuski, S. Maslov, P. Bak, Phys. Rev. E 53 (1996) 414–443.
[67] J. Kempe, Contemp. Phys. 44 (2003) 307–327.